



**HAL**  
open science

## **Failure of bivalve foundation species recruitment related to trophic changes during an extreme heatwave event**

Alana Correia-Martins, Réjean Tremblay, Béatrice Bec, Cécile Roques, Ariane Atteia, Angélique Gobet, Marion Richard, Masami Hamaguchi, Toshihiro Miyajima, Masakazu Hori, et al.

### ► To cite this version:

Alana Correia-Martins, Réjean Tremblay, Béatrice Bec, Cécile Roques, Ariane Atteia, et al.. Failure of bivalve foundation species recruitment related to trophic changes during an extreme heatwave event. *Marine Ecology Progress Series*, 2022, 691, pp.69-82. 10.3354/meps14060 . hal-03700673

**HAL Id: hal-03700673**

**<https://hal.umontpellier.fr/hal-03700673>**

Submitted on 2 Nov 2022

**HAL** is a multi-disciplinary open access archive for the deposit and dissemination of scientific research documents, whether they are published or not. The documents may come from teaching and research institutions in France or abroad, or from public or private research centers.

L'archive ouverte pluridisciplinaire **HAL**, est destinée au dépôt et à la diffusion de documents scientifiques de niveau recherche, publiés ou non, émanant des établissements d'enseignement et de recherche français ou étrangers, des laboratoires publics ou privés.

1 **Failure of bivalve foundation species recruitment related to trophic changes during an**  
2 **extreme heat wave event**

3

4 Alana Correia-Martins<sup>1</sup>, Réjean Tremblay<sup>1</sup>, Béatrice Bec<sup>2</sup>, Cécile Roques<sup>2</sup>, Ariane Atteia<sup>3</sup>,  
5 Angélique Gobet<sup>3</sup>, Marion Richard<sup>3</sup>, Masami Hamaguchi<sup>4</sup>, Toshihiro Miyajima<sup>5</sup>, Masakazu  
6 Hori<sup>4</sup>, Gilles Miron<sup>6</sup>, Stéphane Pouvreau<sup>7</sup>, Franck Lagarde<sup>3\*</sup>

7

8 <sup>1</sup>Institut des sciences de la mer, Université du Québec à Rimouski, 310 allée des Ursulines, G5L  
9 3A1, Rimouski, QC, Canada

10 <sup>2</sup>MARBEC, Univ Montpellier, CNRS, Ifremer, IRD, Montpellier, France

11 <sup>3</sup>MARBEC, Univ Montpellier, CNRS, Ifremer, IRD, Sète, France

12 <sup>4</sup>National Research Institute of Fisheries and Environment of Inland Sea, Fisheries Research  
13 Agency, Maruishi 2-17-5, Hatsukaichi, Hiroshima 739-0452, Japan

14 <sup>5</sup>Marine Biogeochemistry Group, Atmosphere and Ocean Research Institute, University of  
15 Tokyo, Kashiwanoha 5-1-5, Kashiwa, Chiba 277-8564, Japan

16 <sup>6</sup>Département de biologie, Université de Moncton, 18 avenue Antonine-Maillet, E1A 3E9  
17 Moncton, NB, Canada

18 <sup>7</sup>UMR LEMAR 6539, IFREMER, Argenton-en-Landunvez, France

19 \*Corresponding author

20

21 **ABSTRACT**

22 Bivalves are regulators of coastal lagoons and provide a wide range of ecosystem services.  
23 However, coastal lagoons are sensitive to climate change. Our objective was to describe the  
24 drivers of the cascade of ecological events that occurred during a summer heat wave and resulted  
25 in recruitment failure of the oyster *Crassostrea gigas*. Results showed elevated temperature and  
26 salinity caused a shift in planktonic food availability toward smaller taxa. These trophic changes  
27 did not affect food accumulation by oyster larvae or their fatty acid composition but did affect  
28 post-metamorphosis success, as their gill development was not adapted to these small particles.  
29 This resulted in the failure of oyster recruitment and stimulated the development of annelids, a  
30 trophic and spatial competitor that can better ingest small particles. This knowledge suggests  
31 that in the context of marine heat waves, the ecological limits of oyster larvae are narrower than  
32 their physiological limits.

33

34 **KEYWORDS**

35 Climate change, Phenology, Extreme Heat Wave, Bivalves, Pacific Oyster, *Crassostrea gigas*,  
36 Reproduction, Larval Ecology, Cascade of Environmental Effects, Trophic Changes.

37

38 **1. INTRODUCTION**

39 Coastal lagoons provide a wide range of ecosystem services (Chapman 2012, Villamagna et al.  
40 2013, Kermagoret et al. 2019), associated with biodiversity, including bivalves which are of  
41 great ecological interest and high commercial value for some of them. Bivalves also have an  
42 important regulatory functions in the ecosystem thanks to their capacity to extract particles, to  
43 regenerate and store nutrients and to form hard biogenic structures (Smaal et al. 2019). However,  
44 because coastal lagoons are shallow and have limited exchange with the ocean, they are highly  
45 sensitive to eutrophication, heat waves, hypoxia and acidification, as well as to the effects of  
46 global climate change (Lloret et al. 2008, Lu et al. 2018, Thomas et al. 2018). An atmospheric  
47 heat wave is defined as five consecutive days with a maximum temperature 5°C above the 1976-  
48 2005 normal (Jouzel et al. 2014). Summer 2019 was characterized by two heat waves of  
49 exceptional intensity over France, including the Thau Basin, one from June 24 to July 7, the  
50 other from July 21 to 27. The absolute heat record for France (46 °C) was measured in Vérargues  
51 in the Hérault administrative department (Météo-France 2019), which includes the Thau basin.  
52 Marine heatwaves (MHW) are extreme events defined as abrupt but prolonged periods of high  
53 sea surface temperatures that can occur anywhere, at any time (Scannell et al. 2016, Schlegel et  
54 al. 2017, Hobday et al. 2018). High water temperatures increase the metabolic requirements of  
55 bivalves (Filgueira et al. 2016, Thomas & Bacher 2018). Even if temperatures remain within  
56 the species' thermal range, high temperatures combined with salinity and/or food variations, can  
57 negatively impact the life cycle of bivalves (Filgueira et al. 2016).

58  
59 Several studies suggest that global changes are disrupting plankton communities and their  
60 nutritional values by affecting the abundance, size and diversity of primary producers

61 (Klauschies et al. 2012, Sommer et al. 2012, Trombetta et al. 2019). Generally, elevated  
62 temperatures affect phytoplankton cell size with a shift from larger to smaller species (Bec et  
63 al. 2005, Trombetta et al. 2019). Adult bivalves can assimilate small phytoplanktonic particles  
64 (Sonier et al. 2016). However, the efficiency of the capture is regulated by the morphology of  
65 their gills, and is generally low when small particles as picoplankton are present (Rosa et al.  
66 2018). Larvae feed through a less selective velum (Bower & Meyer 1990). Marine  
67 phytoplankton species are major producers of long-chain polyunsaturated essential fatty acids  
68 (EFA) but are predicted to decrease due to ocean warming (Hixson & Arts 2016, Colombo et  
69 al. 2017). The fatty acids docosahexaenoic acid (22:6 $\omega$ 3; DHA), eicosapentaenoic acid (20:5 $\omega$ 3;  
70 EPA) and arachidonic acid (AA) are essential for the growth and survival of marine  
71 invertebrates, particularly during their metamorphosis from pelagic larvae to benthic juveniles  
72 and ultimately, their recruitment success (Gagné et al. 2010, Bassim et al. 2015). Since EFAs  
73 are poorly biosynthesized by marine animals, their intake depends on their food (Glencross  
74 2009, Da Costa et al. 2015). Thus, both the right size and the right fatty acid composition of  
75 larval food are essential for the recruitment success of bivalves.

76 The aim of this study was to identify the environmental factors and trophic conditions  
77 (Supplementary material table1 & table 2) associated with the recruitment failure of the Pacific  
78 oyster, *Crassostrea gigas*, during a heat wave. We compared two contrasted years (2017 no heat  
79 wave and 2019 heat wave) in four sites in the Thau lagoon, France (Fig. 1). We hypothesize that  
80 the heat waves, characterized by high temperatures and high salinity, have a negative impact on  
81 oyster recruitment due to poor larval feeding conditions caused by changes in plankton diversity.

82

## 83 **2. MATERIALS AND METHODS**

84 **2.1 Experimental design**

85 Oyster recruitment was monitored from July 24 to August 21, 2017, and from July 2 to 29, 2019,  
86 at four experimental sites in the Thau lagoon (southern France; Fig 1.). The average depth of  
87 the lagoon is 4 m. The lagoon covers an area of 7 500 ha (19 km x 4.5 km) of which 20% is  
88 used for shellfish culture (oysters and mussels). The lagoon is connected to the Mediterranean  
89 Sea via a network of channels through Sète Harbor(Fiandrino et al. 2017). Two experimental  
90 sites were located inside the shellfish farming areas (Marseillan and Bouzigues) while two  
91 others were located outside the shellfish farming areas (Meze and Listel) (Fig 1.).

92

93 **2.2 Oyster analyses**

94 Three sets of oyster collectors were submerged vertically 2 m below the surface at each of the  
95 four study sites in the Thau lagoon to collect young settlers (pediveligers settled on collectors,  
96 metamorphosed juveniles, and newly metamorphosed juveniles). The collectors were installed  
97 once the oyster's larval supply reached a density of 10 000 larvae/m<sup>3</sup> (VELYGER network<sup>44</sup>).  
98 The collectors located inside the shellfish culture areas were suspended from existing farming  
99 structures. Those outside the area were suspended using a mooring system (Lagarde et al. 2017,  
100 2019). Each collector was made of 44 white PVC plastic plates (15 cm diameter; surface area  
101 of 250 cm<sup>2</sup>) stacked on a 110 cm tube. Two weeks after their immersion, three plates per  
102 collector were harvested [at the top (i.e., the 5<sup>th</sup> from the surface), in the middle (the 22<sup>nd</sup>) and  
103 at the bottom (the 39<sup>th</sup>)] and data were pooled to assess the abundance of young settlers and fatty  
104 acid (FA) content (µg larva<sup>-1</sup>). A similar sampling procedure was used four weeks after the  
105 collectors were immersed to assess the abundance of juveniles.

106 The abundance of young settlers and juveniles was assessed on the upper surface of each plate  
107 using standard 15 cm<sup>2</sup> sub-units. Depending on the abundance, 3 to 12 sub-units were randomly  
108 selected for counting and the resulting replicates were averaged to obtain the total number of  
109 individuals per plate. Recruitment was evaluated from the abundance of juveniles and  
110 metamorphosis from the ratio of juvenile to young-settler abundances. Size at metamorphosis  
111 was estimated by measuring the prodissoconch II (PII) (Martel et al. 1995). A maximum of 60  
112 spats were removed from each plate sampled after the fourth week after immersion, and placed  
113 on a plasticine flange fixed on a microscope blade. Observations were made under the wide-  
114 range zoom lens of a high-resolution digital microscope Keyence (VHX 2000E, 1 μm resolution,  
115 HDR images), and the maximum dorsoventral axis was measured. This measurement  
116 corresponds to the distance between the umbo and the most distant part of the clear demarcation  
117 formed by a growth line delimiting the PII from the dissoconch shell.

118

119 The fatty acid (FA) composition of young settlers was determined using a pool of 77 to 212  
120 individuals per replicate (2-3 replicates per site depending on pediveliger abundances). Samples  
121 were preserved in vials with 3 mL of dichloromethane methanol (CH<sub>2</sub>Cl<sub>2</sub>:MeOH, 2:1 v:v),  
122 closed with a Teflon-lined cap under nitrogen atmosphere and stored at -80 °C until analysis.  
123 Lipids were extracted by grinding in dichloromethane methanol using a modified Folch  
124 procedure (Parrish 1999). Fatty acid methyl esters (FAME) were prepared using sulfuric acid  
125 and methanol (2:98 v:v) at 100 °C for 10 min and using 19:0 as internal standard (Lepage &  
126 Roy 1984). Samples were purified on an activated silica gel with 1 mL of hexane ethyl acetate  
127 (v:v) to eliminate free sterols. FAME were analyzed in the full scan mode (ionic range: 50–650  
128 m:z) on a Polaris Q ion trap coupled to a Trace GC Ultra gas chromatograph (Thermo Scientific)

129 equipped with a TriPlus autosampler, a PTV injector and an ITQ900 mass detector (Thermo  
130 Scientific). An Omegawax 250 (Supelco) capillary column was used for separation using high  
131 purity helium. Xcalibur v.2.1 software (Thermo Scientific) was used for FAME identification  
132 and quantification with the standards (Supelco 37 Component FAME Mix and Supelco  
133 menhaden oil). Unknown peaks were identified according to their mass spectra with emphasis  
134 on FA trophic makers.

135

### 136 **2.3 Environmental measurements**

137 Environmental factors were measured once a week (supplementary files table 1 and table 2) just  
138 after immersion of the collectors until the plates were harvested, i.e., a total of five weeks.  
139 Temperature ( $^{\circ}\text{C}$ ), salinity (PSU) and dissolved oxygen concentrations ( $\text{mg L}^{-1}$ ) were measured  
140 at a depth of 1 m and at the bottom of the water column with an Oxi1970i WTW oximeter and  
141 an LF 197-S WTW conductivity meter.

142

143 Potential food for oysters is expressed as the concentration of total suspended particulate matter  
144 varying in size from 0.7 and 20  $\mu\text{m}$  ( $\text{TPM}_{0.7-20\mu\text{m}}$ ,  $\text{mg L}^{-1}$ ). It consisted of inorganic ( $\text{PIM}_{0.7-20\mu\text{m}}$ ,  
145  $\text{mg L}^{-1}$ ) and organic particulate matter ( $\text{POM}_{0.7-20\mu\text{m}}$ ,  $\text{mg L}^{-1}$ ). Once a week, three replicate water  
146 samples were collected at a depth of 1 m using a Ruttner Standard Water Sampler (Hydro-Bios  
147 Apparatebau) and stored at 4  $^{\circ}\text{C}$  for less than 2 hours before filtration for the measurement of  
148 the concentrations ( $\text{mg mL}^{-1}$ ) of pico and nano-seston. In 2017, 500-mL subsamples of 1-L  
149 samples were used for filtration, while 1-L subsamples of 2-L samples were used in 2019. Water  
150 samples were first filtered by gravity through a Nuclepore membrane (20  $\mu\text{m}$  pore size).  
151 Fractioned water samples were then filtered using a vacuum pressure pump (0.3 bar) on pre-



152 weighed (Mettler Toledo XP6 microbalance) pre-combusted (at 500 °C) Whatman 25 mm GF/F  
153 filters (0.7 µm pore size). The GF/F filters were rinsed with an isotonic seawater solution of  
154 ammonium formate (38 g L<sup>-1</sup> distilled water) to eliminate salt deposits and stored in Millipore™  
155 PetriSlide™ containers at - 25°C. The filters were dried at 70 °C for 24 h, weighed and the  
156 concentration of total particulate matter TPM<sub>0.7-20µm</sub> was determined. The filters were then  
157 combusted at 500 °C for 5 h and reweighed to determine the concentration of particulate  
158 inorganic matter (PIM<sub>0.7-20µm</sub>, mg L<sup>-1</sup>). The concentration of particulate organic matter (POM<sub>0.7-  
159 20µm</sub>, mg L<sup>-1</sup>) was the difference in weight between the dried and the combusted filter. To  
160 determine the FA content of the pico- and nano-seston (µg.mg TPM<sub>0.7-20µm</sub><sup>-1</sup>), 1-L water samples  
161 collected in 2017 and 2-L water samples collected in 2019 were filtered as described above  
162 without addition of ammonium formate solution. GF/F filters were stored in 3 ml of  
163 CH<sub>2</sub>Cl<sub>2</sub>:MeOH (2:1 v:v) under a nitrogen atmosphere in vials with a Teflon-lined cap and stored  
164 at -80 °C. The mass of total fatty acids in the seston (MTFA; µg mg<sup>-1</sup> POM) and its composition  
165 (% fatty acids) were obtained as already described for oysters, with lipid extraction carried out  
166 by sonification rather than grinding.

167

168 Plankton diversity was collected in 1-L samples in 2017 and in 2-L samples in 2019 collected  
169 weekly with a Ruttner Standard Water Sampler (Hydro-Bios Apparatebau) at each sampling  
170 site. This sampling strategy provided 40 observations (4 sites x 5 weeks x 2 years).  
171 Phytoplankton was characterized using the standard Utermöhl method NF-EN-152014, 2006 in  
172 10 mL seawater samples. Abundances are expressed as the number of individuals per liter in 52  
173 diatom taxa and 38 dinoflagellate taxa. Chlorophyll *a* (Chl-*a*), *b* (Chl-*b*) and *c* (Chl-*c*) biomasses  
174 were evaluated in 200 ml seawater samples filtered (Bec et al. 2005, 2011) on Whatman GF/F

175 membranes (0.7  $\mu\text{m}$  pore size) with a vacuum pressure pump (<10 cm Hg). Filters were stored  
176 in glass tubes at -20  $^{\circ}\text{C}$  until analysis. To determine the contribution of picophytoplankton (<3  
177  $\mu\text{m}$ ), nanophytoplankton (3 to 20  $\mu\text{m}$ ) and microphytoplankton (>20  $\mu\text{m}$ ), two out of three  
178 samples were size-fractionated beforehand by gravity through Nuclepore membranes (3 and 20  
179  $\mu\text{m}$  pore size). Filters were ground in acetone (90%) and extracted at 4  $^{\circ}\text{C}$  for 24 h in the dark.  
180 Pigment contents were measured with a spectrofluorometer (Perkin-Elmer LS50b) (Neveux &  
181 Lantoiné 1993) and are expressed in  $\mu\text{g chl } a \text{ L}^{-1}$ . Concentrations of picocyanobacteria (<1  $\mu\text{m}$ ),  
182 autotrophic picoeukaryotes (<3  $\mu\text{m}$ ), nanophytoplankton (3-20  $\mu\text{m}$ ) and bacteria were estimated  
183 using a FACSCalibur flow cytometer Becton Dickinson methods (Marie et al. 1997, Bec et al.  
184 2011). Seawater samples (1-ml) were analyzed; abundances are expressed in cells per liter. Total  
185 picophytoplankton abundances were assessed by summing picocyanobacteria and  
186 photosynthetic picoeukaryote abundances. Fluorescent beads (0.94  $\mu\text{m}$ ; 2 and 3  $\mu\text{m}$ ,  
187 Polysciences) were added to each sample. To measure bacterial abundances, seawater samples  
188 were fixed with prefiltered (0.2  $\mu\text{m}$ ) buffered formaldehyde (2% final concentration) and stored  
189 in liquid nitrogen. The procedure was slightly modified as higher concentrations of  
190 fluorochromes (SYBR Green I) were used (Bouvy et al. 2016). The fixed samples were  
191 incubated with SYBR Green I (Molecular Probes) at a final concentration of 1/375 at 4  $^{\circ}\text{C}$  for  
192 15 min in the dark. Stained bacterial cells excited at 488 nm were determined according to their  
193 side-scattered light and green fluorescence collected using a 530/30 nm filter. Fluorescent beads  
194 (0.94  $\mu\text{m}$ ; Polysciences) were added to each sample.

195 Protozooplankton (heterotrophic flagellates) abundances were determined using the standard  
196 2006 Utermöhl method NF-EN-152014, and are expressed in cells per liter. Until used for  
197 heterotrophic flagellate analysis, 30-ml seawater samples were preserved with 2.5-ml of

198 prefiltered (0.2  $\mu\text{m}$ ) formaldehyde and kept at 4 °C in the dark. Before counting, 10 ml  
199 subsamples were stained with 4',6-diamidino-2-phenylindole (DAPI) for a final concentration  
200 of 2.5  $\mu\text{g ml}^{-1}$ . Heterotrophic flagellates were counted by size class (2-5  $\mu\text{m}$ , 5-10  $\mu\text{m}$  and >10  
201  $\mu\text{m}$ ) under an epifluorescence microscope (Olympus AX70) with UV illumination (Sherr et al.  
202 1993).

203

#### 204 **2.4 Territorial competition**

205 Percent cover of tubeworm (*Ficopomatus enigmaticus*) on plates sampled in the fourth week  
206 after immersion (6 plates per site) was estimated to assess territorial competition with oyster  
207 juveniles, but only during the 2019 sampling season, as no tubeworms were observed in 2017.  
208 Photographs of each plate were taken with a GoPro HERO4 Silver camera equipped with a  
209 macro pro filter (San Mateo, CA, USA) and the % of tubeworms recovered on the plate was  
210 estimated using Image-Pro Insight 9.1 software (MediaCybernetics, Rockville, MD, USA).

211

#### 212 **2.5 Statistical analyses**

213 All PERMANOVA analyses were performed with Primer 7 and Permanova+1 (version 7.0.13)  
214 software. A two-way PERMANOVA (n perm.: 9999) was conducted using a Euclidian distance  
215 matrix to test the effect of year (2 fixed levels) and sampling site (4 fixed levels) on size at  
216 metamorphosis, total and essential fatty acid contents in young settlers and on all the  
217 environmental variables measured, except the oxygen level, which was added as a third factor  
218 (depth) in the analysis. Homogeneity was evaluated using the permutation analysis of  
219 multivariate dispersion (PERMDISP) routine. When significant PERMANOVAs were  
220 observed, post hoc multiple comparison tests were carried out. Multivariate analyses of total

221 FA composition in young settlers and in seston, including *a posteriori* pairwise comparison,  
222 were done using distance-based permutational multivariate analysis of variance  
223 (PERMANOVA, 9999 permutations) based on Euclidian dissimilarities with year (2 fixed  
224 levels) and sampling site (4 fixed levels) as sources of variation. Variations in FA composition,  
225 expressed in percentages, were visualized using non-metric multidimensional scaling (n-MDS).  
226 The similarity percentages (SIMPER) procedure was performed on untransformed data to  
227 identify the FAs that explained the most dissimilarity between significant different levels.

228

### 229 **3. RESULTS**

#### 230 **3.1 Oyster recruitment**

231 Recruitment numbers showed dramatic annual variability with great success at some sites in  
232 2017 but an overall near-zero recruitment level at all sites in 2019 (Fig. 2a, b). In 2017, the  
233 metamorphosis survival rate, expressed as the ratio of juvenile to young settler abundances per  
234 plate, also showed marked spatial variability. The ratio of juvenile ( $123 \pm 9$  ind. plate<sup>-1</sup>) to  
235 young-settler abundances per plate ( $49 \pm 6$  ind. plate<sup>-1</sup>) was 2.5 in Bouzigues, suggesting up to  
236 100% successful metamorphosis by competent larvae and the arrival of competent larvae from  
237 elsewhere. However, in the other sites, recruitment level decreased by 24% ( $94 \pm 16$  juveniles  
238 plate<sup>-1</sup>) in Meze, 90% ( $13 \pm 2$  juveniles plate<sup>-1</sup>) in Listel, and 97% ( $4 \pm 2$  juveniles plate<sup>-1</sup>) in  
239 Marseillan. A poorer supply of larvae ( $6 \pm 2$  young-settlers plate<sup>-1</sup>) was observed in Marseillan,  
240 but the metamorphosis survival rate was 0.6. However, in Meze and Listel, the low recruitment  
241 rates were not linked to the supply of larvae, as young settler abundances were higher in Meze  
242 ( $328 \pm 71$  young settler plate<sup>-1</sup>, with a metamorphosis survival rate of 0.3) and in Listel ( $670 \pm$   
243  $65$  young settler plate<sup>-1</sup>, with a metamorphosis survival rate of 0.02) than in Bouzigues. Failure

244 characterized the 2019 oyster recruitment season: low abundances of young settlers were  
245 observed in Meze ( $116 \pm 5$  ind. plate<sup>-1</sup>) and in Listel ( $31 \pm 2$  ind. plate<sup>-1</sup>), with almost 3 and 22  
246 times fewer individuals than in 2017, respectively. This trend was not observed in Bouzigues  
247 ( $84 \pm 9$  ind. plate<sup>-1</sup>) or in Marseillan ( $45 \pm 3$  ind. plate<sup>-1</sup>) in 2019. Instead, young settlers were  
248 respectively 2 and 7 times higher in 2019 than in 2017. However, two weeks later, almost no  
249 juveniles were observed on the plates (average  $0.14 \pm 0.06$ ), regardless of the sites, pointing to  
250 a general oyster recruitment failure in 2019.

251 The size of juveniles at metamorphosis (PII length) was established in all samples, except  
252 samples from Bouzigues in 2019 (Fig 2c, d), in which no metamorphosis of young settlers to  
253 juveniles was observed. PII individuals sampled in 2019 were 5.1% smaller (mean  $262 \pm 1$   $\mu\text{m}$ )  
254 than those sampled in 2017 (mean  $276 \pm 1$   $\mu\text{m}$ ). Differences among sites were only observed in  
255 2017, when PII sizes in Bouzigues were 2.7% smaller than those in Meze ( $p = 0.02$ ), Listel ( $p$   
256  $= 0.01$ ) and Marseillan ( $p = 0.03$ ).

257 No differences in total fatty acid (TFA) contents were observed in young settlers in the four  
258 sites and the two years. The overall TFA average was  $51 \pm 19$  ng larvae<sup>-1</sup> ( $p > 0.06$ ). The sum of  
259 essential fatty acids (EFA) corresponded to about 10% of TFA with an effect of year  $\times$  site ( $df=3$   
260 and 19, pseudo- $F=6.47$ ,  $p=0.007$ ), as individuals in Listel ( $p=0.02$ ) and Marseillan ( $p=0.006$ )  
261 had 5 times lower TFA contents in 2017 than in 2019. The fatty acid composition of young  
262 settlers varied with the year  $\times$  site interaction ( $df=3$  and 19, pseudo- $F=2.34$ ,  $p=0.017$ ), as  
263 individuals sampled in Listel ( $p=0.047$ ) and Marseillan ( $p=0.044$ ) had different profiles in the  
264 two years (Supplementary material Fig. 1). According to SIMPER analysis, the interannual  
265 differences observed at these two sites were linked to DHA (22:6n3), EPA (20:5n3), AA  
266 (20:4n6), 18:2n6, 18:0 and 16:0 explained more than 83% of the average dissimilarity in the

267 fatty acid profiles. DHA, EPA and AA levels in young settlers sampled in 2019 were twice  
268 higher than in 2017, while the levels of 18:2n6 were five times lower in 2019 than in 2017,  
269 except for the Meze and Bouzigues sites ( $p > 0.09$ ).

270

### 271 **3.2 Physico-chemical parameters**

272 Average water temperatures were 2.6°C higher and salinity was 0.34 S higher in 2019 than in  
273 2017 (Fig 3a, b, Supplementary Table 3 and Supplementary Table 4). A site effect was also  
274 observed for salinity in the Thau lagoon. Salinity increased from east to west: the mean value at  
275 Marseillan was 0.68 S higher than at Bouzigues. Conversely, no effect of site on temperature  
276 was observed. There was a site  $\times$  year effect on oxygen concentration (Supplementary Table 5).  
277 No difference was observed among sites in 2017 (c). The lowest values were observed in  
278 Bouzigues in 2019 ( $p = 0.001$ ) near the bottom of the lagoon (21.8% lower than in 2017).  
279 Oxygen concentrations varied with water depth, lower values generally being observed near the  
280 bottom (Fig. 3c).

281

### 282 **3.3 Potential food for oyster larvae**

283 Concentrations of TPM<sub>0.7-20</sub> (), PIM<sub>0.7-20</sub> () and POM<sub>0.7-20</sub> () were more than twice higher in 2019  
284 than in 2017 (Fig. a, b, c, Supplementary Table 6, 7 and 8). Significant differences among the  
285 four sites were only observed in POM<sub>0.7-20</sub> concentrations. In both years, POM<sub>0.7-20</sub>  
286 concentrations in Marseillan were 0.7 and 0.8 times lower than in Listel and Meze ( $p = 0.01$  and  
287 0.03 respectively). An effect of year  $\times$  chl-*a* biomasses fraction was observed (Supplementary  
288 Table 9). Mean nanophytoplankton and picophytoplankton biomasses ( $p = 0.0001$  and  
289  $p = 0.0004$  respectively) were 3 times higher in 2019 (Fig.4d, e) than in 2017. A site  $\times$  year

290 effect was also observed, chl-*a* biomass values were 45% lower in Bouzigues than in Listel  
291 ( $p=0.01$ ) and Meze ( $p = 0.004$ ) in 2017. In 2019, biomasses in Marseillan were 62% lower than  
292 at the other sites ( $p < 0.02$ ). Interannual variability in chl-*a* was only found in Bouzigues with 3  
293 times more biomass in 2019 ( $p = 0.0007$ ) than in 2017. Similar patterns were observed for chl-  
294 *b* and chl -*c* biomass, with twice as much chl-*b* in the samples collected 2019 samples than in  
295 the samples collected in 2017 ( $0.069 \mu\text{g L}^{-1}$  versus  $0.026 \mu\text{g L}^{-1}$ ;  $p=0.0001$ ), and a more than  
296 two-fold increase in chl-*c* ( $0.103 \text{ ug L}^{-1}$  versus  $0.046 \text{ ug L}^{-1}$ ), particularly in Listel ( $p=0.039$ )  
297 and Bouzigues ( $p=0.0003$ ).

298 Flow cytometry data showed an effect of the year factor on cells smaller than  $3 \mu\text{m}$  (Fig. ).  
299 Abundances of picoeukaryotes ( $<3 \mu\text{m}$ ) (Supplementary Table 10), picocyanobacteria ( $<1 \mu\text{m}$ )  
300 (Supplementary Table 11 and 12) and bacteria (Supplementary Table 14) were higher in 2019  
301 than in 2017. However, nanophytoplankton ( $3\text{-}20 \mu\text{m}$ ) abundances decreased by 39% in 2019  
302 (Supplementary Table 13). The abundance of total heterotrophic flagellates did not vary  
303 significantly among sites or between years, mean value  $2\ 866 \pm 291 \text{ cell mL}^{-1}$ . Dinoflagellate  
304 and diatom abundances were affected by the year factor ( $df=1$  and  $35$ , pseudo- $F=5.64$ ,  $p=0.023$ ),  
305 total values decreased by 60% in 2019 compared to 2017. These variations were linked to a 93%  
306 decrease in *Chaetoceros* abundance from  $184\ 715 \pm 66\ 846$  to  $12\ 483 \pm 3\ 540 \text{ cells L}^{-1}$  (Simper  
307 contribution: 77%,  $df=1$  and  $35$ , pseudo- $F=8.73$ ,  $p=0.0001$ ) and a decrease that led to the  
308 disappearance of *Skeletonema* in Listel and Meze between 2017 and 2019. Diatom taxa were  
309 fewer in number at all sites sampled in 2019 with a maximum of 13 compared to 21 taxa  
310 identified in 2017. A marked increase in *Pseudo-nitzschia* ( $19\ 920 \pm 10\ 513$  to  $50\ 562 \pm 13\ 652$   
311  $\text{cells L}^{-1}$ ) with a Simper contribution of 8% and ( $df=1$  and  $35$ , pseudo- $F=8.73$ ,  $p=0.0001$ ),  
312 *Leptocylindrus* (Simper contribution 7%), *Thalassionema*, and *Cylindrotheca* ( $1\ 837 \pm 222$  to

313 18 712 ± 12 010 cells L<sup>-1</sup>) was observed in 2019 compared to 2017. This trend is especially  
314 expressed in Bouzigues (Fig. 6). This result also reflects the higher diversity of dinoflagellate  
315 taxa observed in 2019 (16 taxa) than in 2017 (12 taxa).

316 TFA contents in the TPM<sub>0.7-20</sub> samples were twice higher in 2019 (19.2 µg mg TPM<sub>0.7-20</sub><sup>-1</sup>) than  
317 in 2017 (9.9 µg mg TPM<sub>0.7-20</sub><sup>-1</sup>; df=1 and 61, pseudo-*F*=17.1, p=0.0002) with no differences  
318 among sites and year × site effects. The fatty acid composition of the TPM<sub>0.7-20</sub> samples differed  
319 between years (df=3 and 76, pseudo-*F*=3.08, p=0.0001; Fig. S2) and, as determined by the  
320 SIMPER analysis, explained 97% of the differences in the levels of 18:1n9, 18:0, 16:1, 18:2n6,  
321 16:0, 14:0, 20:5n3 and 22:6n3. Twenty-six percent of the difference observed between years  
322 was related to 18:1n9, a FA that was twice as abundant in 2017 (up to 24.1% of the TFA)  
323 compared to 2019. The dissimilarity in the FA profiles observed between years was also  
324 explained by higher values of 18:2n6 (representing up to 10.8% of TFA), and EPA (7%) in  
325 2017. 18:2n6 and EPA were, respectively, 11.3% and 5% higher in 2017 than in 2019. The most  
326 abundant FAs in the TPM<sub>0.7-20</sub> samples in 2019 were 16:1 and DHA which explained,  
327 respectively, 13% and 4.3% of the dissimilarity shown by the SIMPER analysis.

328

### 329 **3.4 Territorial competition by worms**

330 The percent cover of tubeworms (*Ficopomatus enigmaticus*) on plates in 2019 showed a marked  
331 increase in this species. Differences were observed among the sites (df=3 and 33, pseudo-  
332 *F*=157, p=0.0001). Results showed similar cover of tubeworms (93.6 ± 1.5%) in Listel and  
333 Bouzigues and a lower cover in Meze (83.2 ± 2.6%) (p < 0.032) and in Marseillan (23.6 ± 3.7%)  
334 (p < 0.0001).

335



#### 4. DISCUSSION

The aim of this study was to identify the environmental and trophic drivers of the decline in the recruitment of the Pacific oyster, *Crassostrea gigas*, in association with a heat wave. Our hypothesis that a heat wave has a negative effect on oyster recruitment by altering plankton diversity was confirmed. While oyster recruitment was normal in 2017, an unprecedented failure was observed in summer 2019 in the Mediterranean Thau lagoon. The atmospheric conditions during a heat wave have a strong direct effects on marine and lagoon environments that supply a variety of ecosystem services and valuable host species (Sarà et al. 2021). Temperature and salinity conditions are key ecological and physiological factors for *Crassostrea* larvae (His et al. 1989b, Baldwin & Newell 1995a, Devakie & Ali 2000, Troost et al. 2009). In controlled experimental settings, the entire larval life of *C. gigas*, including metamorphosis, showed a high tolerance to temperatures ranging from 17 °C to 32 °C at a salinity level of 34, with low mortality ( $\leq 10\%$ ) and the maximum growth rate at 32 °C (Rico-Villa et al. 2009). The physiological limits of temperature tolerance were therefore not reached in our experimental conditions and temperature was not the origin of the failure in this case. Salinity did not drop below 38 in either the 2017 or 2019 recruitment season, and intermittently reached more than 40 in 2019. *Crassostrea gigas* is an estuarine organism that tolerates a wide range of salinity (Nell & Holliday 1988), but no information is available in the literature on the upper salinity tolerance of the larval stage in real conditions. The high salinity in 2019 could represent the physiological salinity threshold for oyster larvae. Our results showed that the larval shell (prodissoconch) at the time of metamorphosis (PII) was smaller in 2019, suggesting a reduction in larval growth or faster achievement of metamorphosis competence in high salinity years. In agreement with Nell and Holliday (1988) who reported an optimal salinity range for larval

359 growth up to 27 and a very marked growth reductions at 31-39 (Nell & Holliday 1988), the  
360 smaller observed\_PII size could be related to growth limitation under high salinity. Interestingly,  
361 these authors reported no significant effect of salinity on larval survival between 19 and 39 but  
362 the growth rate of larvae decreased markedly from 30 S (Helm & Millican 1977). Upper  
363 tolerance limits of oysters to high salinity ranging from 35 S to 45 S should thus be further tested  
364 in the laboratory including interactions with high temperature and different nutritional inputs  
365 (His et al. 1989a).

366 The heat wave that occurred in 2019 resulted in large quantities of particulate matter and  
367 chlorophyll biomass, but their quality appeared to be unfavorable for oyster recruitment. The  
368 failure of oyster recruitment in 2019 could thus be linked to the change in the phytoplankton  
369 community with low abundance of forage diatoms and high abundance of picoplanktonic  
370 prokaryotes and eukaryotes, flagellates, and of the diatoms *Pseudo-Nitzschia* and  
371 *Cylindrotheca*. However, the trophic environment was not characterized by a planktonic  
372 community poor in fatty acids, and it was in fact richer than in 2017. Pediveliger larvae  
373 accumulated the same quantity of fatty acids in 2019 as in 2017, but metamorphosis failures  
374 were observed at all sites. We suggest that this failure may be linked to inappropriate trophic  
375 conditions, which in turn, are mainly linked to the size of picoplankton species. These species  
376 are poorly retained by the newly developed gills of young metamorphosed juveniles. Except for  
377 larvae, the retention efficiency of bivalves for particles < 3-4  $\mu\text{m}$  is low (Baldwin & Newell  
378 1995b, Rosa et al. 2018). Our results suggest that the overabundance of small particles  
379 (picoplanktonic prokaryotes and eukaryotes) could be critical for larval settlement and  
380 metamorphosis. Higher chlorophyll biomass was observed in the nanophytoplankton fraction  
381 during the heat wave of 2019 than in 2017, indicating changes in the phytoplankton community.

382 The heat wave was characterized by the increasing abundances of picocyanobacteria (Bec et al.  
383 2005, Collos et al. 2009, Derolez et al. 2020b) and decreasing abundances of  
384 nanophytoplankton. The Thau lagoon began an oligotrophication trajectory in the early 2000s  
385 (Collos et al. 2009, Derolez et al. 2020a). This process caused a community shift due to a  
386 reduction in nutrient loads since the 1970s thanks to improved wastewater treatment in the  
387 watershed aimed at halting eutrophication (EC 1991a b, 2000). The reduction in nutrient loads  
388 has been amplified by a decrease in total rainfall since the 2000s due to climate change (Derolez  
389 et al. 2020a). Our results corroborate evidence that the proportion of small taxa, like  
390 picoplankton, in the phytoplankton community, is increasing in coastal, marine and freshwater  
391 ecosystems in response to global warming (Daufresne et al. 2009, Mousing et al. 2014, Pinckney  
392 et al. 2015). Small phytoplankton cells have been observed to dominate in oligotrophic  
393 environments (Irwin et al. 2006).

394

395 The high temperatures and high salinity in 2019 had a negative impact on trophic conditions for  
396 larvae. However, recruitment failure appeared to be more linked to the ecological limitations of  
397 the larvae at the time of their metamorphosis than to their physiological state. At the same time,  
398 high temperatures and high salinity stimulated the development of the annelid *Ficopomatus*  
399 *enigmaticus*, triggering a shift in community composition that is destructive for oyster  
400 recruitment. We consequently hypothesize that these annelids are important territorial  
401 competitors (Heiman & Micheli 2010, McQuaid & Griffiths 2014, Peria & Pernet 2019) and  
402 trophic competitors of oyster larvae (Davies et al. 1989, Bruschetti et al. 2008, 2018, Pan &  
403 Marcoval 2014) in shallow water and brackish habitats.

404 This study demonstrates, for the first time, an ecological process leading to the recruitment  
405 failure of the Pacific oysters due to an extreme heat wave. The oligotrophication trajectory of  
406 our study site combined with the effects of high water temperatures promoted variations in the  
407 phytoplankton communities that benefit picophytoplankton including cyanobacteria, that are  
408 likely unfavorable for the successful larval development of oysters until their juvenile  
409 metamorphosis (Lagarde et al. 2017). The present study thus reveals the ecological limits of the  
410 reproductive process of the Pacific oyster in the context of a heat wave in a Mediterranean  
411 lagoon. The heat wave phenomenon observed in 2019 severely disrupted the reproductive cycle  
412 of oysters in the Thau lagoon. In this context, the oyster nursery function within an oyster  
413 farming ecosystem can only be achieved or maintained when pico-, nano- and  
414 microphytoplankton communities are present and abundant and oysters can find favorable areas  
415 for larval development and optimize their recruitment. This study provides evidence that, in the  
416 conditions caused by a heat wave, the ecological limits of Pacific oyster larvae are narrower  
417 than their physiological limits. The effects of climate change, particularly the warming of waters  
418 in semi-enclosed basins, will certainly lead to problems in larval harvesting in the near futures.  
419 The information presented in this paper should help adapt oyster aquaculture, including  
420 husbandry practices, to a future marked by climate change.

## 421 **5. Data and code availability**

422 All data used in the current study and scripts used in our analysis are publicly available or were  
423 obtained by the corresponding author. This research benefited from the VELYGER Database:  
424 The Oyster Larvae Monitoring French Project (<http://doi.org/10.17882/41888>) and REPHY

425 Dataset - French Observation and Monitoring program for Phytoplankton and Hydrology in  
426 coastal waters. Metropolitan data. SEANOE (<https://doi.org/10.17882/47248>).

427

## 428 **6. REFERENCES**

429 Baldwin BS, Newell RI (1995a) Feeding rate responses of oyster larvae (*Crassostrea virginica*)  
430 to seston quantity and composition. J Exp Mar Bio Ecol 189:77–91.

431 Baldwin BS, Newell RI (1995b) Relative importance of different size food particles in the  
432 natural diet of oyster larvae (*Crassostrea virginica*). Mar Ecol Prog Ser 120:135–146.

433 Bassim S, Chapman RW, Tanguy A, Moraga D, Tremblay R (2015) Predicting growth and  
434 mortality of bivalve larvae using gene expression and supervised machine learning. Comp  
435 Biochem Physiol - Part D Genomics Proteomics 16:59–72.

436 Bec B, Collos Y, Souchu P, Vaquer A, Lautier J, Fiandrino A, Benau L, Orsoni V, Laugier T  
437 (2011) Distribution of picophytoplankton and nanophytoplankton along an anthropogenic  
438 eutrophication gradient in French Mediterranean coastal lagoons. Aquat Microb Ecol  
439 63:29–45.

440 Bec B, Husseini-Ratrema J, Collos Y, Souchu P, Vaquer A (2005) Phytoplankton seasonal  
441 dynamics in a Mediterranean coastal lagoon: Emphasis on the picoeukaryote community.  
442 J Plankton Res 27:881–894.

443 Bouvy M, Got P, Domaizon I, Pagano M, Leboulanger C, Bouvier C, Carre C, Roques C, Dupuy  
444 C (2016) Plankton communities in the five Iles Eparses (Western Indian Ocean) considered  
445 to be pristine ecosystems. Acta oecologica- Int J Ecol 72:9–20.

446 Bower SM, Meyer SG (1990) Atlas of anatomy and histology of larvae and early juvenile stages  
447 of Japanese scallop *Patinopecten yessoensis*. Can Spec Publ Fish Aquat Sci 111:1–51.

448 Bruschetti CM, Addino M, Luppi T, Iribarne O (2018) Effects of nutrient enrichment and  
449 grazing by an invasive filter feeder on phytoplankton biomass in a South West Atlantic  
450 coastal lagoon. *Biol Invasions* 20:2245–2256.

451 Bruschetti M, Luppi T, Fanjul E, Rosenthal A, Iribarne O (2008) Grazing effect of the invasive  
452 reef-forming polychaete *Ficopomatus enigmaticus* (Fauvel) on phytoplankton biomass in  
453 a SW Atlantic coastal lagoon. *J Exp Mar Bio Ecol* 354:212–219.

454 Chapman PM (2012) Management of coastal lagoons under climate change. *Estuar Coast Shelf*  
455 *Sci* 110:32–35.

456 Collos Y, Bec B, Jauzein C, Abadie E, Laugier T, Lautier J, Pastoureaud A, Souchu P, Vaquer  
457 A (2009) Oligotrophication and emergence of picocyanobacteria and a toxic dino fl  
458 agellate in Thau lagoon , southern France. *J Sea Res* 61:68–75.

459 Colombo SM, Wacker A, Parrish CC, Kainz MJ, Arts MT (2017) A fundamental dichotomy in  
460 long-chain polyunsaturated fatty acid abundance between and within marine and terrestrial  
461 ecosystems. *Environ Rev* 25:163–174.

462 Da Costa F, Robert R, Quéré C, Wikfors GH, Soudant P (2015) Essential Fatty Acid  
463 Assimilation and Synthesis in Larvae of the Bivalve *Crassostrea gigas*. *Lipids* 50:503–  
464 511.

465 Daufresne M, Lengfellner K, Sommer U (2009) Global warming benefits the small.

466 Davies BR, Stuart V, de Villiers M (1989) The filtration activity of a serpulid polychaete  
467 population *Ficopomatus enigmaticus* (Fauvel) and its effects on water quality in a coastal  
468 marina. *Estuar Coast Shelf Sci* 29:613–620.

469 Derolez V, Malet N, Fiandrino A, Lagarde F, Richard M, Ouisse V, Bec B, Aliaume C (2020a)  
470 Fifty years of ecological changes: Regime shifts and drivers in a coastal Mediterranean

471 lagoon during oligotrophication. *Sci Total Environ* 732:139292.

472 Derolez V, Soudant S, Malet N, Chiantella C, Richard M, Abadie E, Aliaume C, Bec B (2020b)

473 Two decades of oligotrophication: evidence for a phytoplankton community shift in the

474 coastal lagoon of Thau (Mediterranean Sea, France). *Estuar Coast Shelf Sci*:106810.

475 Devakie MN, Ali AB (2000) Salinity-temperature and nutritional effects on the setting rate of

476 larvae of the tropical oyster, *Crassostrea iredalei* (Faustino). *Aquaculture* 184:105–114.

477 EC (1991a) Council Directive 91/271/EEC Concerning Urban Waste-water Treatment.

478 EC (1991b) Council Directive 91/676/EEC of 12 December 1991 Concerning the Protection of

479 Waters against Pollution Caused by Nitrates from Agricultural Sources.

480 EC (2000) Directive 2000/60/EC of the European Parliament and of the Council of 23 October

481 2000 Establishing a Framework for Community Action in the Field of Water Policy.

482 Fiandrino A, Ouisse V, Dumas F, Lagarde F, Pete R, Malet N, Le Noc S, de Wit R (2017)

483 Spatial patterns in coastal lagoons related to the hydrodynamics of seawater intrusion. *Mar*

484 *Pollut Bull* 119:132–144.

485 Filgueira R, Guyondet T, Comeau LA, Tremblay R (2016) Bivalve aquaculture-environment

486 interactions in the context of climate change. *Glob Chang Biol* 22:3901–3913.

487 Gagné R, Tremblay R, Pernet F, Miner P, Samain JF, Olivier F (2010) Lipid requirements of

488 the scallop *Pecten maximus* (L.) during larval and post-larval development in relation to

489 addition of *Rhodomonas salina* in diet. *Aquaculture* 309:212–221.

490 Glencross BD (2009) Exploring the nutritional demand for essential fatty acids by aquaculture

491 species. 71–124.

492 Heiman KW, Micheli F (2010) Non-native Ecosystem Engineer Alters Estuarine Communities.

493 *Integr Comp Biol* 50:226–236.

494 Helm MM, Millican PF (1977) Experiments in the hatchery rearing larvae. 11.

495 His E, Robert R, Dinet A (1989a) Combined effect of temperature and salinity on fed and  
496 starved larvae of the Mediterranean mussel *Mytilus galloprovincialis* and the Japanese  
497 oyster *Crassostrea gigas*. Mar Biol 100:455–463.

498 His E, Robert R, Dinet A (1989b) Marine Biology of the Mediterranean mussel *Mytilus*  
499 *galloprovincialis* and the Japanese oyster *Crassostrea gigas*. Mar Biol 100:455–463.

500 Hixson SM, Arts MT (2016) Climate warming is predicted to reduce omega-3, long-chain,  
501 polyunsaturated fatty acid production in phytoplankton. Glob Chang Biol 22:2744–2755.

502 Hobday AJ, Oliver ECJ, Gupta A Sen, Benthuisen JA, Burrows MT, Donat MG, Holbrook NJ,  
503 Moore PJ, Thomsen MS, Wernberg T, Smale DA (2018) Categorizing and Naming Marine  
504 Heatwaves. Oceanography 31:162–173.

505 Irwin AJ, Finkel ZOE V, Schofield OME, Falkowski PG (2006) Scaling-up from nutrient  
506 physiology to the size-structure of phytoplankton communities. 28.

507 Jouzel J, Ouzeau G, Déqué M, Jouini M, Planton S, Vautard R (2014) Le climat de la France au  
508 XXI<sup>e</sup> siècle (Volume 4), Scénarios régionalisés: édition 2014 pour la métropole et les  
509 régions d’outre-mer.

510 Kermagoret C, Claudet J, Derolez V, Nugues MM, Ouisse V, Quillien N, Baulaz Y, Le Mao P,  
511 Scemama P, Vaschalde D, Bailly D, Mongruel R (2019) How does eutrophication impact  
512 bundles of ecosystem services in multiple coastal habitats using state-and-transition  
513 models. Ocean Coast Manag 174:144–153.

514 Klausches T, Bauer B, Aberle-Malzahn N, Sommer U, Gaedke U (2012) Climate change  
515 effects on phytoplankton depend on cell size and food web structure. Mar Biol 159:2455–  
516 2478.



517 Lagarde F, Fiandrino A, Ubertini M, Roque d'Orbcastel E, Mortreux S, Chiantella C, Bec B,  
518 Bonnet D, Roques C, Bernard I, Richard M, Guyondet T, Pouvreau S, Lett C (2019)  
519 Duality of trophic supply and hydrodynamic connectivity drives spatial patterns of Pacific  
520 oyster recruitment. *Mar Ecol Prog Ser* 632:81–100.

521 Lagarde F, Roque E, Ubertini M, Mortreux S, Bernard I, Fiandrino A, Chiantella C, Bec B,  
522 Roques C, Bonnet D, Miron G, Richard M, Pouvreau S, Lett C, Marbec IUMR (2017)  
523 Recruitment of the Pacific oyster *Crassostrea gigas* in a shellfish-exploited Mediterranean  
524 lagoon : discovery, driving factors and a favorable environmental window. *Mar Ecol Prog*  
525 *Ser* 578:1–17.

526 Lepage G, Roy CC (1984) Improved recovery of fatty acid through direct transesterification  
527 without prior extraction or purification. *J Lipid Res* 25:1391–1396.

528 Lloret J, Marín A, Marín-Guirao L (2008) Is coastal lagoon eutrophication likely to be  
529 aggravated by global climate change ? 78.

530 Lu Y, Yuan J, Lu X, Su C, Zhang Y, Wang C, Cao X, Li Q, Su J, Ittekkot V, Garbutt RA, Bush  
531 S, Fletcher S, Wagey T, Kachur A, Sweijd N (2018) Major threats of pollution and climate  
532 change to global coastal ecosystems and enhanced management for sustainability. *Environ*  
533 *Pollut* 239:670–680.

534 Marie D, Partensky F, Jacquet S, Vaulot D (1997) Enumeration and cell cycle analysis of natural  
535 populations of marine picoplankton by flow cytometry using the nucleic acid stain SYBR  
536 Green I. *Appl Environ Microbiol* 63:186–193.

537 Martel A, Hynes TMT, Buckland-Nicks J (1995) Prodissoconch morphology, planktonic shell  
538 growth, and site at metamorphosis in *Dreissena polymorpha*. *Can J Zool* 73:1835–1844.

539 McQuaid KA, Griffiths CL (2014) Alien reef-building polychaete drives long-term changes in

540 invertebrate biomass and diversity in a small, urban estuary. *Estuar Coast Shelf Sci*  
541 138:101–106.

542 Météo-France (2019) 46,0 °C à Vérargues : nouveau record officiel de température observée en  
543 France. [http://www.meteofrance.fr/actualites/74345599-c-est-officiel-on-a-atteint-les-46-](http://www.meteofrance.fr/actualites/74345599-c-est-officiel-on-a-atteint-les-46-c-en-france-en-juin)  
544 [c-en-france-en-juin](http://www.meteofrance.fr/actualites/74345599-c-est-officiel-on-a-atteint-les-46-c-en-france-en-juin)

545 Mousing EA, Ellegaard M, Richardson K (2014) Global patterns in phytoplankton community  
546 size structure — evidence for a direct temperature effect. *497:25–38*.

547 Nell JA, Holliday JE (1988) Effects of Salinity on the Growth and Survival of Sydney Rock  
548 Oyster (*Saccostrea commercialis*) and Pacific Oyster (*Crassostrea gigas*) Larvae and Spat.  
549 68:39–44.

550 Neveux J, Lantoiné F (1993) Spectrofluorometric assay of chlorophylls and phaeopigments  
551 using the least squares approximation technique. *Deep Res Part I 40:1747–1765*.

552 Pan J, Marcoval MA (2014) Top-Down Effects of an Exotic Serpulid Polychaete on Natural  
553 Plankton Assemblage of Estuarine and Brackish Systems in the SW Atlantic. *J Coast Res*  
554 30:1226–1235.

555 Parrish CC (1999) Determination of Total Lipid, Lipid Classes, and Fatty Acids in Aquatic  
556 Samples. *Lipids Freshw Ecosyst:4–20*.

557 Peria J, Pernet B (2019) Tolerance to salinity and thermal stress by larvae and adults of the  
558 serpulid annelid *Ficopomatus enigmaticus*. *Invertebr Biol 138:e12271*.

559 Pinckney JL, Benitez-Nelson CR, Thunell RC, Muller-Karger F, Lorenzoni L, Troccoli L,  
560 Varela R (2015) Phytoplankton community structure and depth distribution changes in the  
561 Cariaco Basin between 1996 and 2010. *Deep Sea Res Part I Oceanogr Res Pap 101:27–37*.

562 Rico-Villa B, Pouvreau S, Robert R (2009) Influence of food density and temperature on

563 ingestion, growth and settlement of Pacific oyster larvae, *Crassostrea gigas*. *Aquaculture*  
564 287:395–401.

565 Rosa M, Ward JE, Shumway SE (2018) Selective Capture and Ingestion of Particles by  
566 Suspension-Feeding Bivalve Molluscs: A Review. *J Shellfish Res* 37:727–746.

567 Sarà G, Giommi C, Giacoletti A, Conti E, Mulder C, Mangano MC (2021) Multiple climate-  
568 driven cascading ecosystem effects after the loss of a foundation species. *Sci Total Environ*  
569 770:144749.

570 Scannell HA, Pershing AJ, Alexander MA, Thomas AC, Mills KE (2016) Frequency of marine  
571 heatwaves in the North Atlantic and North Pacific since 1950. *Geophys Res Lett* 43:2069–  
572 2076.

573 Schlegel RW, Oliver ECJ, Wernberg T, Smit AJ (2017) Nearshore and offshore co-occurrence  
574 of marine heatwaves and cold-spells. *Prog Oceanogr* 151:189–205.

575 Sherr EB, Caron DA, Sherr BF (1993) Staining of heterotrophic protists for visualization via  
576 epifluorescence microscopy. In: *Handbook of Methods in Aquatic Microbial Ecology*, 1st  
577 Editio. Kemp PF, Sherr BF, Sherr EB, Cole JJ (eds) Lewis Publishers, p 213–227

578 Smaal AC, Ferreira JG, Grant J, Petersen JK, Strand Ø (2019) Goods and Services of Marine  
579 Bivalves.

580 Sommer U, Adrian R, Bauer B, Winder M (2012) The response of temperate aquatic ecosystems  
581 to global warming: novel insights from a multidisciplinary project. *Mar Biol* 159:2367–  
582 2377.

583 Sonier R, Filgueira R, Guyondet T, Tremblay R, Olivier F, Meziane T, Starr M, LeBlanc AR,  
584 Comeau LA (2016) Picophytoplankton contribution to *Mytilus edulis* growth in an  
585 intensive culture environment. *Mar Biol* 163:1–15.

586 Thomas Y, Bacher C (2018) Assessing the sensitivity of bivalve populations to global warming  
587 using an individual-based modelling approach. *Glob Chang Biol*:1–18.

588 Thomas Y, Cassou C, Gernez P, Pouvreau S (2018) Oysters as sentinels of climate variability  
589 and climate change in coastal ecosystems. *Environ Res Lett* 13.

590 Trombetta T, Vidussi F, Mas S, Parin D, Simier M, Mostajir B (2019) Water temperature drives  
591 phytoplankton blooms in coastal waters. *PLoS One* 14:1–28.

592 Troost K, Gelderman E, Kamermans P, Smaal AC, Wolff WJ (2009) Effects of an increasing  
593 filter feeder stock on larval abundance in the Oosterschelde estuary (SW Netherlands). *J*  
594 *Sea Res* 61:153–164.

595 Villamagna AM, Angermeier PL, Bennett EM (2013) Capacity, pressure, demand, and flow: A  
596 conceptual framework for analyzing ecosystem service provision and delivery. *Ecol*  
597 *Complex* 15:114–121.

598

## 599 **7. ACKNOWLEDGEMENTS**

600 This research was supported by the Natural Sciences and Engineering Research Council of  
601 Canada (NSERC-Discovery Grant no.299100) to R.T and by the *Ressources Aquatiques Québec*  
602 *Research Network (Fonds de Recherche du Québec-Nature et Technologies, #2014-RS-*  
603 *171172)* and MITACS (FR37656) for the internships of ACM during her stay at IFREMER.  
604 This research was also fund by the VELYGER network. F.L. and R.T. thank the RECHAGLO  
605 international research group, co-funded by Ifremer and the Department of Fisheries and Oceans  
606 (DFO), and the *Institut France-Québec pour la coopération scientifique en appui au secteur*  
607 *Maritime (IFQM)* for encouragement, support, and exchanges with Canada. F.L., M.H. T.M.

608 and M.H. thank FREA, JSPS and Campus France/Ministry of Foreign Affairs for funding the  
609 scientific exchange needed for this study and the development of all the ideas presented by our  
610 group.

611 We thank H el ene Cochet, Serge Mortreux, Ana ıs Crottier, Clarisse Hubert, Nabila Guenineche,  
612 Gabriel Devique, Herv e Violette, Elise Hatey, Camille Gianaroli and Nathalie Gauthier for  
613 logistic support in the field and technical contributions in the laboratory.

614

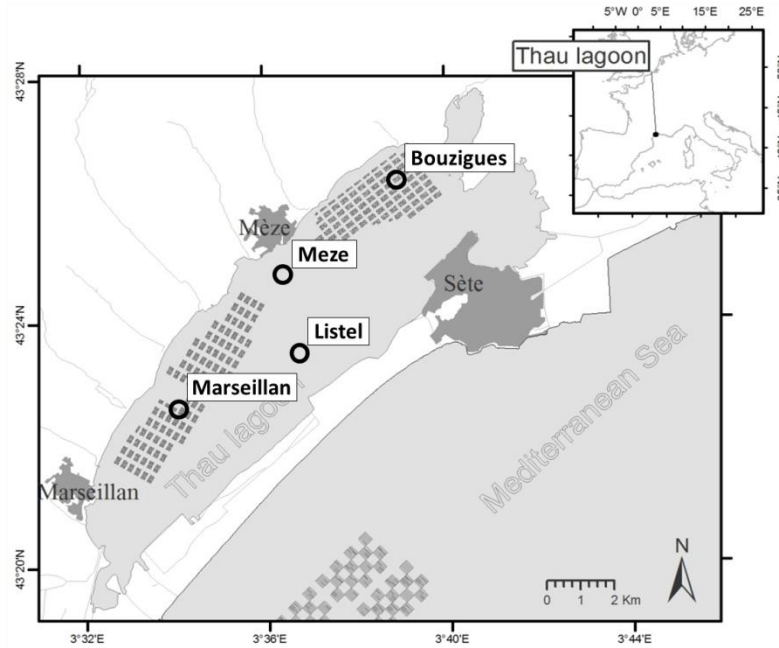
## 615 **8. AUTHOR CONTRIBUTIONS**

616 A.C.M. was involved in investigation, methodology, writing, data curation, formal analysis, and  
617 visualization. R.T. and F.L. were involved in conceptualization, funding acquisition,  
618 investigation, methodology, writing, data curation, formal analysis, visualization, and project  
619 administration. S.P. was involved in conceptualization, funding acquisition, investigation,  
620 methodology, writing and project administration. B.B was involved in conceptualization,  
621 funding acquisition, investigation, methodology, writing, data curation, formal analysis, and  
622 visualization. C.R. contributed to funding acquisition, methodology, writing, data curation and  
623 formal analysis. A.A and A.G. contributed to writing and interpretation. G.M. contributed to  
624 funding acquisition, investigation, methodology, writing and formal analysis. M.R., M.Ho,  
625 M.Ha. and T.M. contributed to conceptualization, investigation, methodology and writing.

## 626 **9. COMPETING INTERESTS**

627 The authors declare no competing interests.

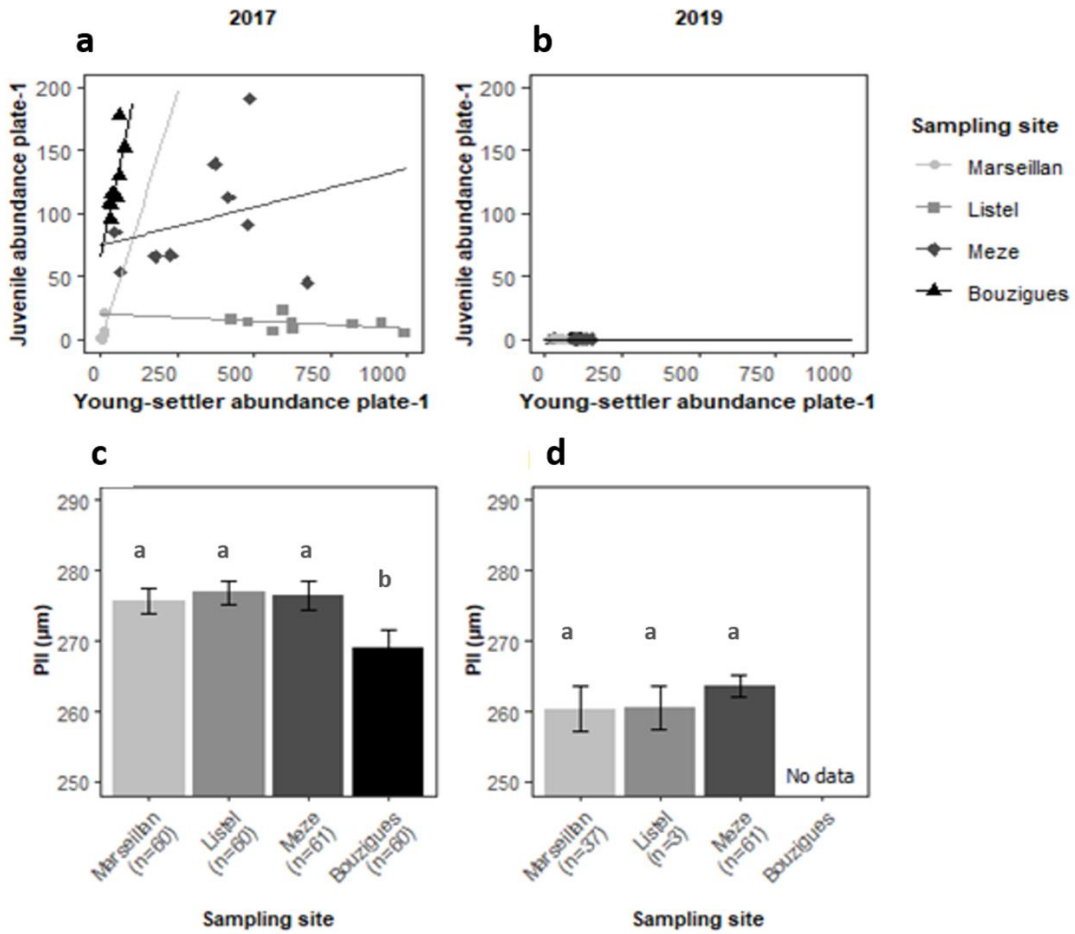
628



629

630 Fig. 1. The four sampling sites in the Thau lagoon. Marseillan and Bouzigues are located in the  
 631 shellfish farming area; shaded areas indicate the location of shellfish culture areas. Meze and  
 632 Listel are located outside the aquaculture area.

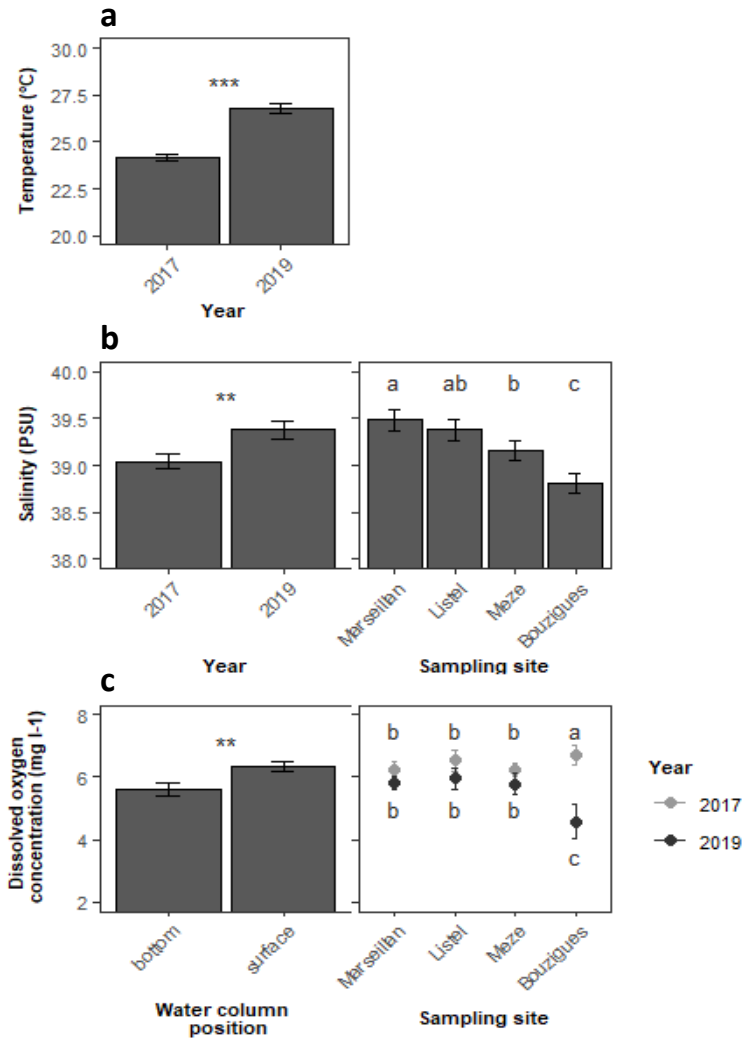
633



634

635 Fig. 2. Variability of oyster recruitment and prodissoconch II size according to the years 2017  
 636 (no heat wave) and 2019 (heat wave). *Crassostrea gigas* recruitment performance with young  
 637 settlers (pediveligers + post-larvae) and juvenile abundance per collector plate observed at the  
 638 four sampling sites during the summer recruitment events in (a) 2017 and in (b) 2019. Size at  
 639 metamorphosis was estimated by the length of prodissoconch II shell (PII,  $\mu\text{m} \pm \text{SE}$ ) of juveniles  
 640 sampled in (c) 2017 and (d) 2019. Different letters indicate significant differences between sites  
 641 according to post-hoc multiple comparison tests after PERMANOVA.

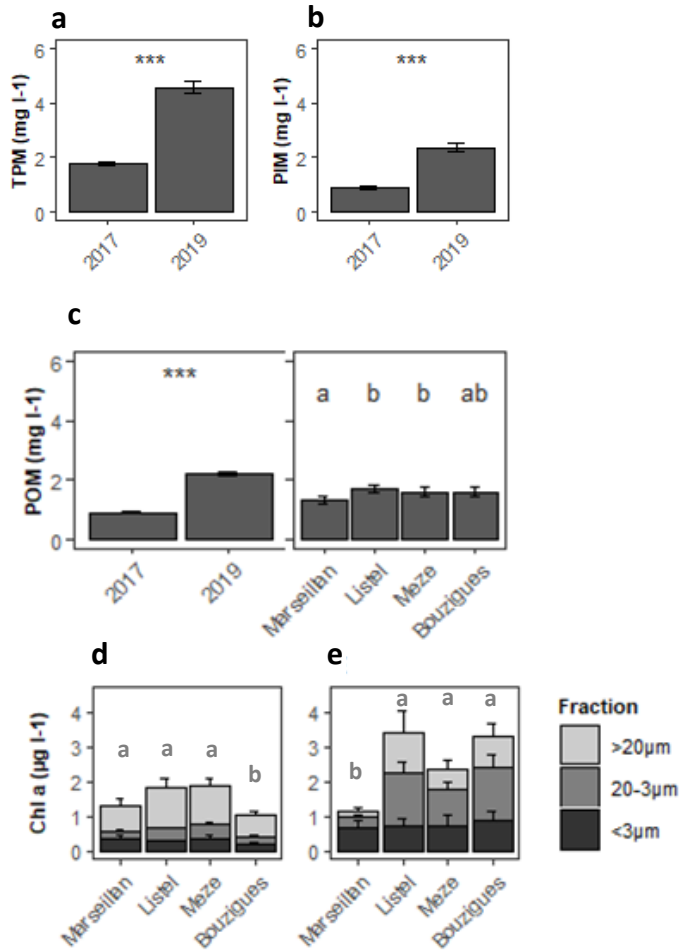
642



643

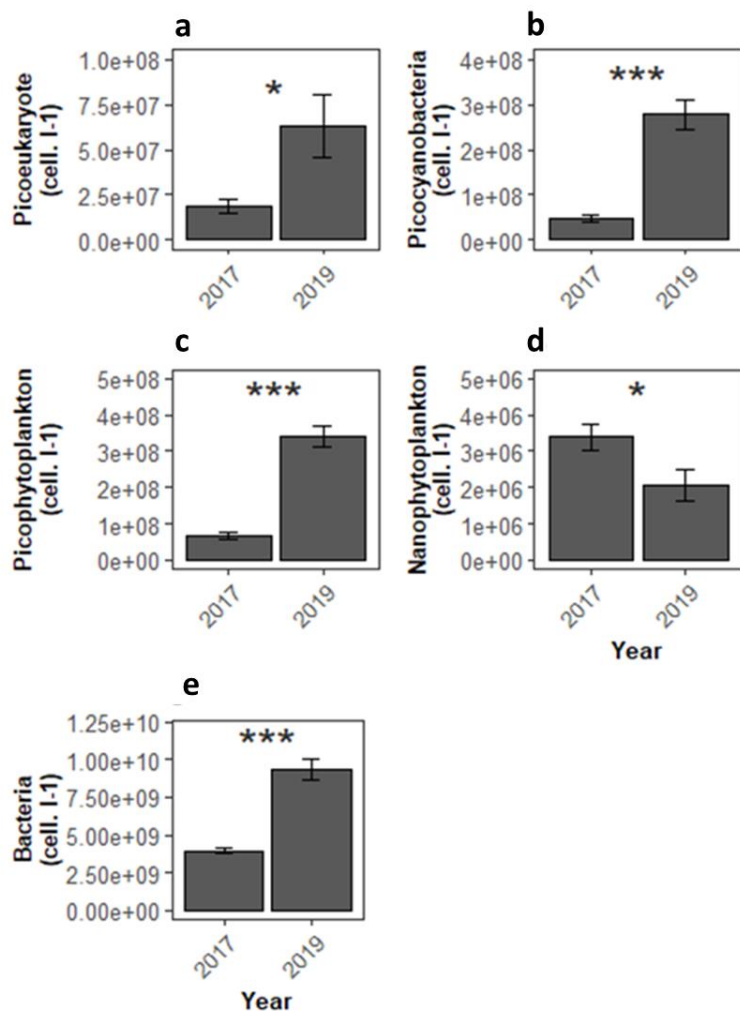
644 Fig. 3. Physico-chemical monitoring in 2017 (no heat wave) and 2019 (heat wave). (a) Mean  
 645 temperature ( $^{\circ}\text{C} \pm \text{SE}$ ) per year ( $n = 40$ ), (b) mean salinity ( $\text{PSU} \pm \text{SE}$ ) per year ( $n = 40$ ) and per  
 646 sampling site ( $n = 20$ ) and (c) mean dissolved oxygen concentration ( $\text{mg L}^{-1} \pm \text{SE}$ ) according to  
 647 the position of the sample in the water column ( $n = 40$ ) and per year and sampling site ( $n = 10$ ).  
 648 Stars indicate significant differences in parameter average per year (\*  $p \leq 0.05$ , \*\*  $p \leq 0.01$ , \*\*\*  
 649  $p \leq 0.001$ ). Different letters indicate significant differences between sites according to post hoc  
 650 multiple comparison tests after PERMANOVA.





651

652 Fig. 4. Hydrobiological monitoring in 2017 (no heat wave) and 2019 (heat wave). Mean  
 653 concentrations of (a) total particulate matter (TPM, mg L<sup>-1</sup> ± SE), (b) particulate inorganic  
 654 matter (PIM, mg L<sup>-1</sup> ± SE) and (c) particulate organic matter (POM, mg L<sup>-1</sup> ± SE) per year and  
 655 sampling site (n = 5 per sampling site and year). Mean concentrations of chlorophyll-a (d, 2017  
 656 and e; 2019; µg L<sup>-1</sup> ± SE), found in the picophytoplankton fraction (< 3 µm), the  
 657 nanophytoplankton fraction (3 to 20 µm) and the microphytoplankton fraction (> 20 µm) per  
 658 year and sampling site (n = 5 per sampling site, year and phytoplankton fraction). Stars indicate  
 659 significant differences according to parameter average by year (\* p ≤ 0.05, \*\* p ≤ 0.01, \*\*\* p ≤  
 660 0.001). Different letters indicate significant differences between sites according to post-hoc  
 661 multiple comparison tests after PERMANOVA.



663

664 Fig. 5: Monitoring of picophytoplankton population in 2017 (no heat wave) and 2019 (heat

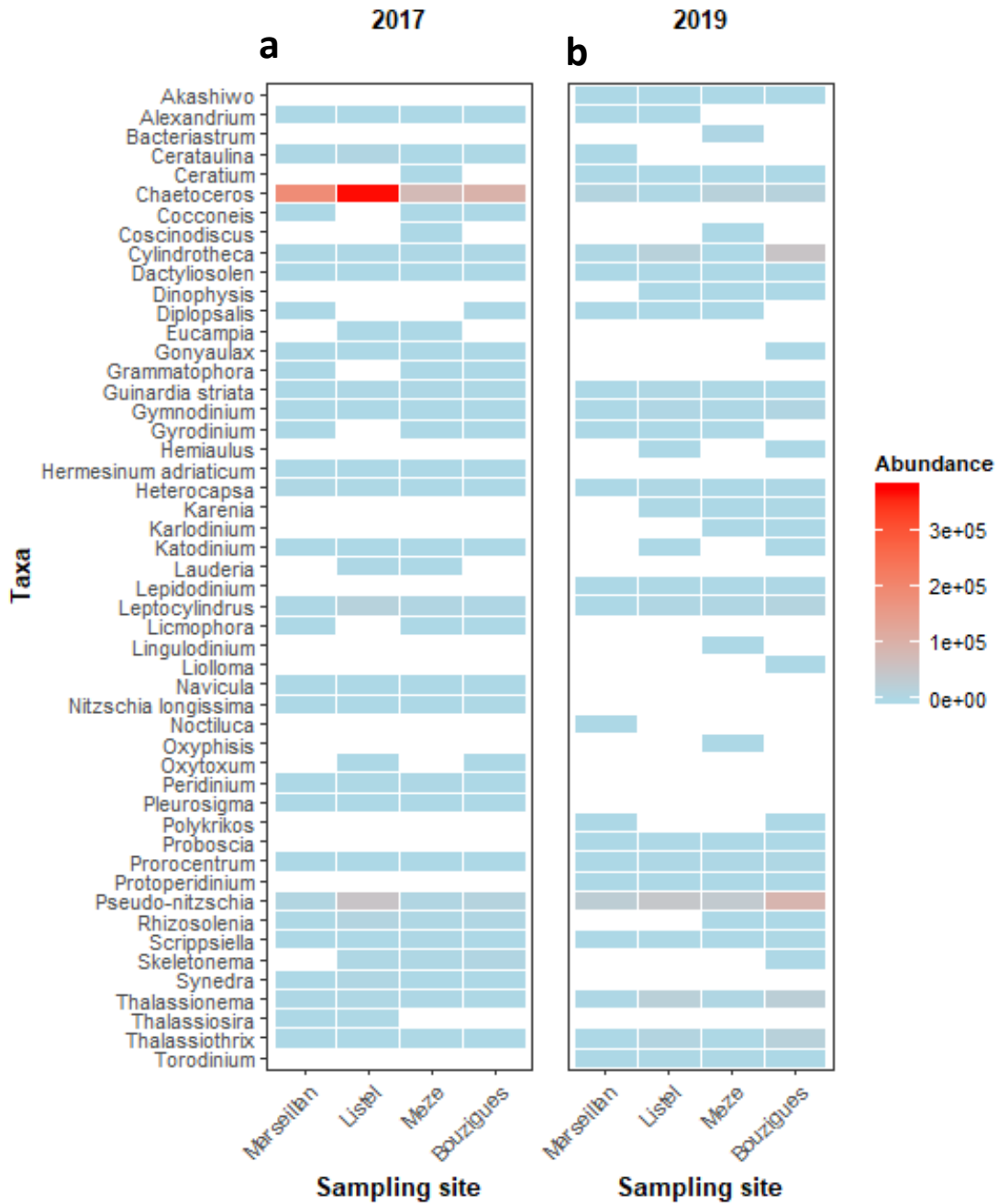
665 wave). Average abundances for all sites of (a) photosynthetic picoeukaryotes, (b)

666 picocyanobacteria, (c) picophytoplankton, (d) nanophytoplankton and (e) bacteria (cells L<sup>-1</sup> ±

667 SE) per year (n=20). Stars indicate significant differences according to parameter average by

668 year (\* p ≤ 0.05, \*\* p ≤ 0.01, \*\*\* p ≤ 0.001).

669



670

671 Fig. 6: Heatmap of microphytoplankton genera with changes in abundances in 2017 (no heat  
 672 wave) and 2019 (heat wave). Average phytoplankton abundance (cells L<sup>-1</sup>) per taxon and  
 673 sampling site in (a) 2017 (n = 5) and (b) in 2019 (n = 4).  
 674

<b>Variables</b>	<b>Description</b>	<b>Unit of measure</b>	<b>Abbreviation</b>
<b><i>Oyster variables</i></b>			
<i>Oyster pediveligers</i>	<i>Abundance on collector plates</i>	<i>ind. plate-1</i>	<i>pediveligers</i>
<i>Newly metamorphosed juveniles</i>	<i>Abundance on collector plates</i>	<i>ind. plate-1</i>	<i>postlarvae</i>
<i>Young settlers</i>	<i>Abundance of pediveligers+ newly metamorphosed juveniles on collector plates</i>	<i>ind. plate-1</i>	<i>Young settlers</i>
<i>Prodissoconch II size</i>	<i>Measurement of prodissoconch maximum shell height along maximal dorsoventral axis of larvae or juvenile Pacific oysters</i>	<i>mm</i>	<i>PII size</i>
<i>Total fatty acid in young settlers</i>	<i>Total fatty acid contents in larvae (young settlers)</i>	<i>ng larvae-1</i>	<i>TFA</i>
<i>Essential fatty acids</i>	<i>Sum of essential fatty acids in larvae (docosahexaenoic acid (22:6<math>\omega</math>3; DHA), eicosapentaenoic acid (20:5<math>\omega</math>3; EPA) and arachidonic acid (AA))</i>	<i>ng larvae-1</i>	<i>EFA</i>

<b>Variables</b>	<b>Description</b>	<b>Unity</b>	<b>Abbreviation</b>
<b>Environmental variables</b>			
Temperature	Discrete measure	°C	-
Salinity	Discrete measure	No unit	-
Oxygen concentration	Discrete measure	mg l <sup>-1</sup>	-
Total particulate matter <sub>0.7-20µm</sub>	Total particular pelagic material in the 0.7-20µm fraction	mg l <sup>-1</sup>	TPM <sub>0.7-20µm</sub>
Particulate organic matter <sub>0.7-20µm</sub>	Particulate pelagic material in fraction the 0.7-20µm fraction	mg l <sup>-1</sup>	POM <sub>0.7-20µm</sub>
Particulate inorganic matter <sub>0.7-20µm</sub>	Particulate inorganic pelagic material in the fraction 0.7-20µm fraction	mg l <sup>-1</sup>	PIM <sub>0.7-20µm</sub>
TFA content in TPM <sub>0.7-20</sub>	TFA content in TPM <sub>0.7-20</sub>	µg mg TPM <sub>0.7-20</sub> <sup>-1</sup>	
Total chlorophyll a	Total chlorophyll a biomass	µgChla l <sup>-1</sup>	chloa
Total chlorophyll b	Total chlorophyll b biomass	µgChlb l <sup>-1</sup>	chl ob
Total chlorophyll c	Total chlorophyll c biomass	µgChlc l <sup>-1</sup>	chl oc
Picophytoplankton biomass	Chlorophyll a biomass in the <3µm fraction (picoeukaryotes)	µgChla l <sup>-1</sup>	pico_chloa
Nanophytoplankton biomass	Chlorophyll a biomass in the 3-20µm fraction (nanoeukaryotes)	µgChla l <sup>-1</sup>	nano_chloa
Picophytoplankton+nanophytoplankton	Biomass	µgChla l <sup>-1</sup>	nano_total_chloa
Microphytoplankton > 20µm	Biomass (microeukaryotes)	µgChla l <sup>-1</sup>	micro_chloa
Bacteria	Abundance of picocyanobacteria (<1 µm)	10 <sup>6</sup> cell. l <sup>-1</sup>	bacteria
Total picoeukaryotes	Abundance	10 <sup>6</sup> cell. l <sup>-1</sup>	peuk_tot
picoeukaryotes+cyanophyceae	Abundance	10 <sup>6</sup> cell. l <sup>-1</sup>	pico_tot
Nanophytoplankton	Abundance	10 <sup>6</sup> cell. l <sup>-1</sup>	nano
cryptophyceae	Abundance	10 <sup>6</sup> cell. l <sup>-1</sup>	crypto
Nanophytoplankton + cryptophyceae	Abundance	10 <sup>6</sup> cell. l <sup>-1</sup>	nano_tot
Heterotrophic flagellates	Abundance	cell l <sup>-1</sup>	HF
Ciliates	Abundance	cell l <sup>-1</sup>	ciliates
Tintinnidae	Abundance	cell l <sup>-1</sup>	tinti
Diatoms	Abundance	cell l <sup>-1</sup>	diatom
Dinoflagellates	Abundance	cell l <sup>-1</sup>	Dinoflagellate
<b>Territorial competition by worms</b>			
Worm coverage	Percent cover of tubeworms ( <i>Ficopomatus enigmaticus</i> ) on plates	%	-

680 *Supplementary Table 3: multivariate PERMANOVA investigating site and year effect for Temperature*

Source	df	SS	MS	Pseudo-F	P(perm)	Unique perms	P(MC)
site	3	7,087	2,3623	1,158	0,3305	9951	0,3335
year	1	135,72	135,72	66,53	0,0001	9825	0,0001
position	1	3,2	3,2	1,5686	0,2085	9805	0,217
sitexyear	3	0,3865	0,12883	0,063154	0,9764	9951	0,9754
sitexposition	3	2,573	0,85767	0,42042	0,7357	9950	0,7371
yearxposition	1	1,1045	1,1045	0,54142	0,4681	9828	0,473
sitexyearxposition	3	0,0865	0,028833	0,014134	0,9977	9955	0,9977
Res	64	130,56	2,04				
Total	79	280,72					

693 *Supplementary Table 4: multivariate PERMANOVA investigating site, depth and year effect for salinity*

Source	df	SS	MS	Pseudo-F	P(perm)	Unique perms	P(MC)
Site	3	5,331	1,777	7,5677	0,0002	9962	0,0004
Year	1	2,2445	2,2445	9,5587	0,0031	9805	0,0034
position	1	0,072	0,072	0,30663	0,5764	9733	0,5827
sitexyear	3	0,5245	0,17483	0,74457	0,5286	9960	0,5323
sitexposition	3	0,059	0,019667	0,083755	0,9666	9945	0,9679
yearxposition	1	0,1125	0,1125	0,47911	0,4824	9806	0,4966
sitexyearxposition	3	0,0805	0,026833	0,11428	0,9545	9942	0,9503
Res	64	15,028	0,23481				
Total	79	23,452					

706 *Supplementary Table 5: multivariate PERMANOVA investigating site, depth and year effect for oxygen*

Source	df	SS	MS	Pseudo-F	P(perm)	Unique perms	P(MC)
site	3	3,8333	1,2778	1,3099	0,2739	9944	0,27
year	1	15,878	15,878	16,277	0,0004	9825	0,0001
position	1	10,039	10,039	10,292	0,002	9854	0,0018
sitexyear	3	10,01	3,3366	3,4205	0,0215	9947	0,0217
sitexposition	3	3,8499	1,2833	1,3156	0,2758	9955	0,2805
yearxposition	1	3,3048	3,3048	3,388	0,0708	9812	0,0682
sitexyearxposition	3	1,7959	0,59865	0,6137	0,6012	9955	0,5985
Res	64	62,43	0,97547				
Total	79	111,14					

719 *Supplementary Table 6: multivariate PERMANOVA investigating site and year effect for TPM*

Source	df	SS	MS	Pseudo-F	P(perm)	Unique perms	P(MC)
site	3	1,493	0,49767	0,28089	0,8424	9962	0,8364
year	1	207,48	207,48	117,1	0,0001	9839	0,0001
sitexyear	3	2,0244	0,67479	0,38085	0,7691	9958	0,7708
Res	100	177,18	1,7718				
Total	107	388,6					

728 *Supplementary Table 7: multivariate PERMANOVA investigating site and year effect for PIM*

Source	df	SS	MS	Pseudo-F	P(perm)	Unique perms	P(MC)
site	3	0,11747	0,039156	0,039431	0,9901	9949	0,9904
year	1	54,939	54,939	55,325	0,0001	9814	0,0001
sitexyear	3	0,33001	0,11	0,11077	0,957	9958	0,9508
Res	100	99,303	0,99303				
Total	107	154,73					

736

737  
738  
739  
740  
741  
742  
743  
744  
745  
746  
747  
748  
749  
750  
751  
752  
753  
754  
755  
756  
757  
758  
759  
760  
761  
762  
763  
764  
765  
766  
767  
768  
769  
770  
771  
772  
773  
774  
775  
776  
777  
778  
779  
780  
781  
782  
783  
784  
785

Supplementary Table 8: multivariate PERMANOVA investigating site and year effect for POM

Source	df	SS	MS	Pseudo-F	P(perm)	Unique perms	P(MC)
site	3	1,4638	0,48793	2,796	0,0429	9952	0,0407
year	1	48,888	48,888	280,15	0,0001	9824	0,0001
sitexyear	3	1,193	0,39765	2,2787	0,0834	9952	0,0832
Res	100	17,451	0,17451				
Total	107	69,327					

Supplementary Table 9: multivariate PERMANOVA investigating site, size and year effect for CHLOA

Source	df	SS	MS	Pseudo-F	P(perm)	Unique perms	P(MC)
site	3	3,35	1,1167	3,9887	0,0088	9958	0,0088
year	1	3,6519	3,6519	13,045	0,0003	9848	0,0007
taille	2	1,8257	0,91286	3,2608	0,0401	9953	0,0456
sitexyear	3	2,9083	0,96945	3,4629	0,0167	9953	0,0175
sitexsize	6	1,984	0,33066	1,1811	0,3199	9933	0,3246
yearxsize	2	5,0665	2,5333	9,0488	0,0004	9951	0,0004
sitexyearxsize	6	0,84964	0,14161	0,50582	0,8156	9949	0,8092
Res	96	26,876	0,27995				
Total	119	46,512					

Supplementary Table 10: multivariate PERMANOVA investigating site and year effect for PEUK\_TOT

Source	df	SS	MS	Pseudo-F	P(perm)	Unique perms	P(MC)
site	3	1,2885E+16	4,2951E+15	1,3441	0,2784	9945	0,2768
year	1	1,959E+16	1,959E+16	6,1306	0,0155	9835	0,0187
sitexyear	3	2,6684E+15	8,8948E+14	0,27835	0,8512	9952	0,8401
Res	32	1,0226E+17	3,1955E+15				
Total	39	1,374E+17					

Supplementary Table 11: multivariate PERMANOVA investigating site, size and year effect for CYAN

Source	df	SS	MS	Pseudo-F	P(perm)	Unique perms	P(MC)
site	3	2,552E+16	8,5068E+15	0,7044	0,5664	9949	0,5635
year	1	5,3384E+17	5,3384E+17	44,205	0,0001	9851	0,0001
sitexyear	3	1,2146E+16	4,0486E+15	0,33524	0,8082	9953	0,797
Res	32	3,8645E+17	1,2077E+16				
Total	39	9,5796E+17					

Supplementary Table 12: multivariate PERMANOVA investigating site, size and year effect for PICO

Source	df	SS	MS	Pseudo-F	P(perm)	Unique perms	P(MC)
site	3	2,3685E+15	7,8951E+14	0,083154	0,9729	9939	0,9697
year	1	7,5797E+17	7,5797E+17	79,832	0,0001	9841	0,0001
sitexyear	3	3,7254E+15	1,2418E+15	0,13079	0,9431	9944	0,938
Res	32	3,0383E+17	9,4946E+15				
Total	39	1,0679E+18					

786

*Supplementary Table 13 : multivariate PERMANOVA investigating site, size and year effect for NANO*

787

Source	df	SS	MS	Pseudo-F	P(perm)	Unique perms	P(MC)
site	3	1,2396E+12	4,1319E+11	0,13497	0,9421	9944	0,9377
year	1	1,7765E+13	1,7765E+13	5,8032	0,0196	9837	0,0175
sitexyear	3	2,0028E+13	6,6759E+12	2,1807	0,1051	9950	0,1082
Res	32	9,7961E+13	3,0613E+12				
Total	39	1,3699E+14					

794

795

*Supplementary Table 14 : multivariate PERMANOVA investigating site, size and year effect for BACT\_TOT*

796

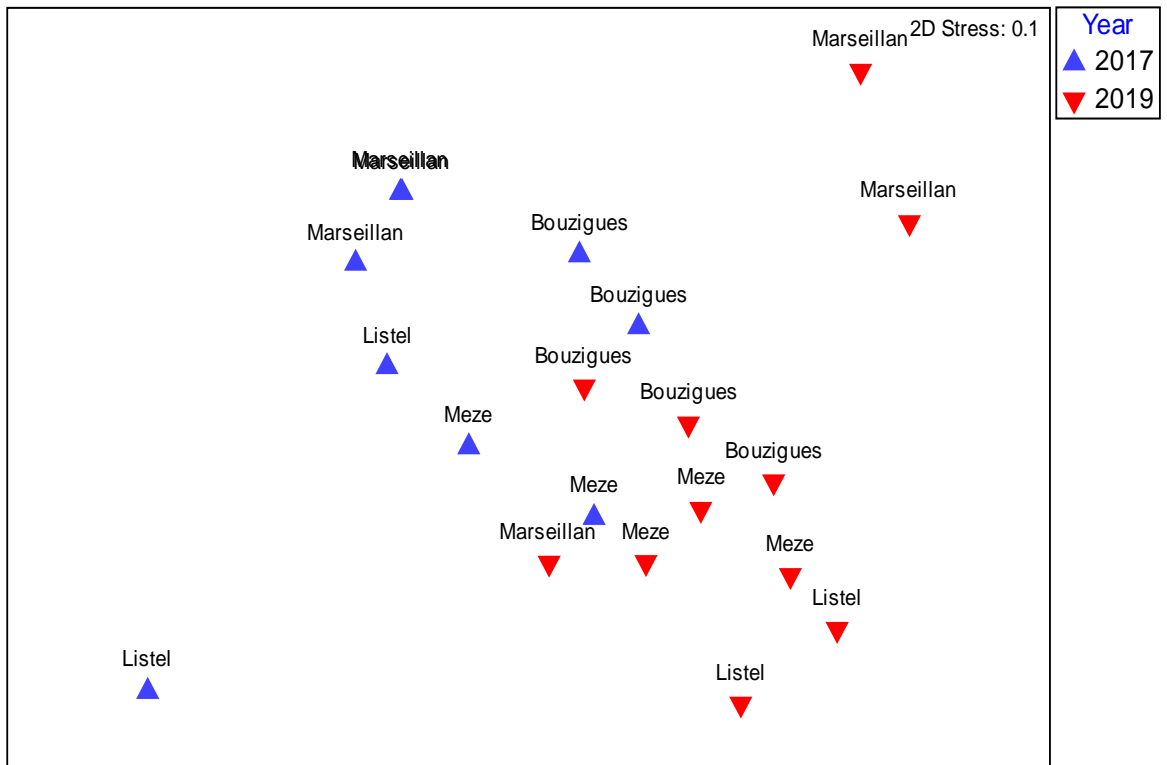
Source	df	SS	MS	Pseudo-F	P(perm)	Unique perms	P(MC)
site	3	1,622E+19	5,4066E+18	0,93657	0,4508	9949	0,4387
year	1	2,909E+20	2,909E+20	50,392	0,0001	9839	0,0001
sitexyear	3	1,0607E+19	3,5358E+18	0,61249	0,6213	9957	0,6151
Res	32	1,8473E+20	5,7728E+18				
Total	39	5,0246E+20					

803

804



Non-metric MDS



805

806 *Supplementary Figure 1. Non-metric multi-dimensional scaling of the Euclidean similarity matrix based on the relative*  
807 *abundance of fatty acid profiles measured in young settlers larvae collected in 2017 and 2019 at each sampling sites in the*  
808 *Thau lagoon.*

809